Neurosci. Bull. February, 2016, 32(1):51–60
DOI 10.1007/s12264-015-0005-6

www.neurosci.cn
www.springer.com/12264

ORIGINAL ARTICLE

Association of Optic Radiation Integrity with Cortical Thickness in Children with Anisometropic Amblyopia

Shun Qi[1,2] · Yun-Feng Mu[3] · Long-Biao Cui[1] · Rong Li[4] · Mei Shi[3] · Ying Liu[1] · Jun-Qing Xu[1] · Jian Zhang[5] · Jian Yang[2] · Hong Yin[1]

Received: 16 July 2015 / Accepted: 9 November 2015 / Published online: 14 January 2016

Abstract Previous studies have indicated regional abnormalities of both gray and white matter in amblyopia. However, alterations of cortical thickness associated with changes in white matter integrity have rarely been reported. In this study, structural magnetic resonance imaging and diffusion tensor imaging (DTI) data were obtained from 15 children with anisometropic amblyopia and 15 age- and gender-matched children with normal sight. Combining DTI and surface-based morphometry, we examined a potential linkage between disrupted white matter integrity and altered cortical thickness. The fractional anisotropy (FA) values in the optic radiations (ORs) of children with anisometropic amblyopia were lower than in controls ($P < 0.05$). The cortical thickness in amblyopic children was lower than controls in the following subregions: lingual cortex, lateral occipitotemporal gyrus, cuneus, occipital lobe, inferior parietal lobe, and temporal lobe ($P < 0.05$, corrected), but was higher in the calcarine gyrus ($P < 0.05$, corrected). Node-by-node correlation analysis of changes in cortical thickness revealed a significant association between a lower FA value in the OR and diminished cortical thickness in the following subregions: medial lingual cortex, lateral occipitotemporal gyrus, lateral, superior, and medial occipital cortex, and lunate cortex. We also found a relationship between changes of cortical thickness and white matter OR integrity in amblyopia. These findings indicate that developmental changes occur simultaneously in the OR and visual cortex in amblyopia, and provide key information on complex damage of brain networks in anisometropic amblyopia. Our results also support the hypothesis that the pathogenesis of anisometropic amblyopia is neurodevelopmental.

Keywords Optic radiation · Cortical thickness · Diffusion tensor imaging · Anisometropic amblyopia · Children

Shun Qi, Yun-Feng Mu and Long-Biao Cui have contributed equally to this work.

✉ Jian Yang
yj1118@mail.xjtu.edu.cn

✉ Hong Yin
yinhong@fmmu.edu.cn

1 Department of Radiology, Xijing Hospital, Fourth Military Medical University, Xi'an 710032, China

2 Department of Radiology, The First Affiliated Hospital of Xi'an Jiaotong University, Xi'an 710061, China

3 Department of Radiotherapy, Xijing Hospital, Fourth Military Medical University, Xi'an 710032, China

4 Department of Ophthalmology, The Affiliated Hospital of Xi'an Medical University, Xi'an 710077, China

5 Department of Respiratory Medicine, Xijing Hospital, Fourth Military Medical University, Xi'an 710032, China

Introduction

Amblyopia is characterized by the developmental impairment of spatial vision, which cannot be corrected by eye refractive instruments. Largely a cortical disorder, it may result from abnormal visual experience in early childhood [1, 2]. It is accepted that a central rather than a retinal deficit is the major factor in the pathogenesis of amblyopia. Animal studies suggest that amblyopia represents functional and morphological influences of visual deprivation on the lateral geniculate nucleus (LGN) and visual cortex [3, 4]. However, the neuroanatomical information on structural changes in the human brain remains limited and inconclusive. Previous neuroimaging studies commonly

focused on adults with amblyopia [5–7] and studies concerning the development of the visual system in children with amblyopia are scarce.

That the visual cortex plays a critical role in the pathogenesis of amblyopia has been confirmed using various techniques, and reduced functional activation in the calcarine cortex has been found [8]. The reduced contrast sensitivity (pattern vision) in amblyopia is coupled with deactivation in identified areas of the occipital visual system [9], and magnetoencephalographic responses in the occipital cortex triggered through the amblyopic eye have longer latencies and smaller amplitudes [10]. Electrophysiological studies have also shown that the visual cortical response to stimulation at higher spatial frequencies is reduced in anisometropic amblyopia [11]. Global brain gray matter [12], including the visual cortex [13], has been investigated physiologically and psychopathologically using functional magnetic resonance imaging (fMRI). Furthermore, recent fMRI studies have shown that amblyopia is associated with deactivation in the striate cortex (Brodmann area 17), the occipitotemporal cortex, and the LGN [14, 15]. In addition, the gray matter volume of the visual cortex is reduced in adults and children with amblyopia, as revealed by voxel-based morphometry (VBM) [16]. However, it has been pointed out that VBM may cause inaccurate assessment in regions of cortical overlap [17]. Surface-based morphometry is feasible to precisely quantify and characterize the cortical thickness in different regions [18–20]. By using this method, comparison of the cortical thickness in the four lateral occipital regions (the medial lingual cortex, the cuneus, the superior occipital cortex and the lunate cortex) showed that these regions are significantly thinner in amblyopic patients than in controls [7].

Diffusion tensor imaging (DTI) reflects water diffusion anisotropy in axons to provide insight into the geometric organization of the white matter. DTI-based diffusion tensor tractography (DTT) can non-invasively provide quantitative structural and functional information on the white matter *in vivo* and is widely used to evaluate white matter integrity [21]. During brain maturation, the total water content declines as myelination develops. Because these maturational processes result in changes of water diffusion, information on the magnitude and severity of any alterations in anisotropy may be important for understanding the pathophysiological features of developmental abnormalities [22, 23]. The integrity of the optic radiation (OR) fibers that are directly connected with the visual cortex also plays an important role in amblyopia. Fractional anisotropy (FA), an imaging measure derived from DTI data, can be used to assess the directionality of molecular diffusion. It has been applied to investigate the maturity and plasticity of white matter fiber tracts [24]. A recent study on amblyopia combined the DTI and DTT techniques and found clear reductions in the FA values of visual fiber tracts in amblyopic patients [25, 26]. Furthermore, the integrity of visual fiber tracts is compromised in amblyopia [5, 6]. The depicted three major bundles of ORs (the anterior, central, and posterior bundles) by the fiber-tracking method were in good agreement with the classic anatomic topography of the visual pathway [27]. In light of the results from previous studies, it may be hypothesized that changes in the visual fiber tracts elicited by amblyopia are associated with abnormalities of the visual cortex. It has been found that the anatomical connections of the OR constrains the fMRI response of the visual cortex [28]. However, the relationship between the thickness of the visual cortex and the integrity of the OR in children with anisometropic amblyopia has not been studied.

In this study, we used surface-based morphometry and DTT to investigate the relationship between cortical thickness and OR integrity in amblyopia. Since the OR fibers are directly connected with the visual cortex, clarifying this correlation may help understand the developmental mechanism of amblyopia.

Participants and Methods

Participants

All participants were recruited from the Ophthalmology Clinic at Xijing Hospital, Fourth Military Medical University, Xi'an, China. Anisometropic amblyopia was defined as 1.5 diopter (D) spherical and/or 1.0 D cylindrical refractive error difference and a best-corrected visual acuity <16/20 according to the established standard of prevention and control for amblyopia and strabismus [29]. Normal acuity was defined as 20/20 or better. The exclusion criteria were: (1) a known organic brain disorder, (2) specific clinical evidence of neurological dysfunction, (3) congenital or acquired organic pathology of the eye, or (4) long-term treatment of the eye. Fifteen children with anisometropic amblyopia and fifteen gender- and age-matched healthy controls were recruited; all were right-handed. In the patient group, the best-corrected visual acuity of the amblyopic eye ranged from 2/20 to 10/20 and that of the other eye from 16/20 to 20/20. In the control group (children with normal vision), the visual acuity of both eyes was 20/20 or better. The controls were recruited from primary schools based in the surrounding area. They all underwent comprehensive examination of the eye to ensure normal acuity and no neurological problems.

All participants were given MRI and DTI scans. This study was approved by the Ethics Committee of the Fourth Military Medical University. Written informed consent was given by all participants before entering the study.

MRI Data Acquisition

All participants wore headphones with their eyes closed and lay in a supine position. They were imaged using the 12-channel head coil of a 3.0-Tesla MR scanner (Magnetom Trio, Siemens AG, Erlangen, Germany) in a dim scanning room. Form padding was used to limit head movement. Each participant received two types of scan. A high-resolution three-dimensional magnetization-prepared rapid acquisition gradient-echo (MPRAGE) T1-weighted sequence was used to acquire MRI data from the whole brain (176 sagittal slices). The MRI parameters were as follows: TR = 1900 ms, TE = 2.26 ms, TI = 900 ms, flip angle = 9°, acquisition matrix = 256 × 256, FOV = 220 mm, slice thickness = 1.00 mm, inter-slice gap = 0 mm, isotropic resolution = 1.0 × 1.0 × 1.0 mm^3, total time = 7 min and 37 s. DTI was acquired using single-shot diffusion-weighted echo-planar imaging (DW-EPI) with the following acquisition parameters: TR = 6100 ms, TE = 71.1 ms, matrix = 128 × 128, FOV = 240 mm × 240 mm, slice thickness = 3 mm, gradient directions = 20, b values = 0 s/mm^2 and 1000 s/mm^2, total time = 7 min and 51 s.

Cortical Thickness Estimation

Cortical reconstruction and parcellation were performed with the FreeSurfer V4 package (v 4.0.2) image analysis suite [30], which is documented and available at http://surfer.nmr.mgh.harvard.edu/. This method has been fully described [31] and validated *via* both histological and manual measurements [32, 33]. For cortical analysis, the gray/white matter interface in each hemisphere was segmented, tessellated, corrected for topological errors, and inflated to unfold the cortical surface. Then, each individual hemispheric surface was registered to a template based on a surface with its sulco-gyral pattern to allow inter-individual analysis [30]. Cortical thickness was calculated from both intensity gradients across tissue class and continuity information, as the closest distance between the gray/white matter border and the gray/cerebrospinal fluid interface at each vertex of the tessellated surface [30]. Automated topology correction was performed as necessary [34]. The cortical thickness values were obtained from the statistical output of FreeSurfer cortical parcellation, called "aparc.a2005s.stats", using the Desikan-Killiany atlas and containing 75 regions. The data from each participant were resampled to an average participant, and a 'qcache' command and 10-mm full-width half-maximum Gaussian kernel were used to perform surface smoothing prior to statistical analysis.

DTI Data Processing

DTT was processed using TrackVis software (http://www.trackvis.org/), which can visualize and analyze fiber tract data from DTI [35]. The mean FA values of the ORs were calculated. The OR fiber bundles were identified on the RGB (red–green–blue) map, using anatomical atlases obtained from children with anisometropic amblyopia and controls. In the RGB map, five ROIs were selected from the bilateral ORs to measure the mean FA values. Each ROI area was designed for 9 pixels uniformly and placed symmetrically in both ORs as described in previous studies [36–38]. Fibers were clustered into bundles using the normalized cut algorithm. A pairwise distance matrix between all fibers was required for clustering. The distance between fibers was defined as the mean of the closest point distances of all points along each fiber. A mean 3D curve attributed with tensors representing average tensors calculated within cross-sections was used to model each bundle. The number of tracks of ORs longer than the mean length (43.24 mm) was used as the coordinate system for statistical analysis.

Statistical Analysis

Cortical Thickness Analysis

QDEC software (https://surfer.nmr.mgh.harvard.edu/fswiki/Qdec), which is a FreeSurfer application, was used to explore the differences in cortical thickness between groups. Group differences were shown *via* statistical parametric maps of the entire cortical mantle. A general linear model was estimated at each vertex across the cortical surface, with cortical thickness as dependent variable, gender as a categorical predictor, and age as a continuous predictor. The mean regional cortical thickness value was obtained for further Pearson correlation analysis between cortical thickness and the FA values of the ORs.

Correlations between DTI and Cortical Thickness

To investigate the correlations of mean FA values for ORs with cortical thickness in amblyopic children, the extracted mean regional cortical thickness and FA value were imported into SPSS 17.0 software (SPSS Inc., Chicago, IL) for Pearson correlation analyses, and the critical level for statistical significance was set at $P < 0.05$ adjusted for multiple comparisons using false discovery rate correction according to the nine clusters with reduced cortical thickness for which correlations were performed (P level adjusted to <0.028) [39].

Table 1 Clinical characteristics of amblyopic children

Participant	Age (years)	Sex	AE	Distance Acuity (logMAR)		Refractive Error		SS	PEP	Microdeviations	OA
				Left	Right	Left	Right				
1	8.1	M	OD	0.03	1	0D	+4.50D	>60″	eso	5△	6
2	6.5	M	OS	0.15	0.8	+2.00D	+0.5D	<60″	ortho	0	5
3	6.5	F	OS	0.1	1	+2.25D	0D	<60″	ortho	0	5
4	7.2	F	OS	0.2	1	+1.5D	0D	<60″	ortho	0	6
5	8.9	F	OS	0.03	0.9	+4.00D	+0.25D	>60″	eso	5△	5
6	6.5	M	OD	0.3	0.9	+0.25D	+1.75D	<60″	ortho	0	6
7	7.3	M	OD	0.1	1	0D	+2.00D	<60″	exo	2△	4
8	9.5	F	OS	0.2	1	+1.25D	0D	<60″	eso	2△	7
9	8.7	M	OD	0.2	1	0D	+1.5D	<60″	ortho	0	5
10	6.5	F	OS	0.15	0.8	+2.25D	+0.5D	<60″	exo	5△	6
11	9.5	F	OD	0.05	1	0D	+3.5D	>60″	exo	5△	6
12	8.5	M	OS	0.2	0.75	+2.0D	+0.75D	<60″	eso	1△	5
13	7.3	M	OS	0.3	1	+1.5D	0D	<60″	ortho	0	5
14	10.3	M	OD	0.1	1	0D	+2.25D	<60″	exo	2△	8
15	9.1	M	OD	0.2	1	0D	+1.50D	<60″	ortho	0	6

AE, amblyopic eye; OD, right eye; OS, left eye; eso, esotropic; exo, exotropic; ortho, orthotropic; SS, stereo score; OA, age at onset of amblyopia; PEP, presence and extent of phoria.

Results

Clinical Data

There were no significant differences between groups in gender (children with anisometropic amblyopia: male/female, 9/6; normal children: 8/7; $\chi^2 = 0.136$, $P = 0.7125$), age (8.0 ± 1.3; 7.9 ± 0.8; $P = 0.8176$), or handedness (right/left: 15/0; 15/0) (nonparametric tests). The detailed demographical characteristics and clinical data are listed in Table 1.

Brain Imaging Results

Cortical Thickness

There was no significant group difference in the whole-brain average cortical thickness. But the children with anisometropic amblyopia showed significantly lower cortical thickness than controls in the following sub-regions of both cerebral hemispheres: medial lingual cortex, lateral occipitotemporal gyrus, lateral occipital cortex, cuneus, superior occipital cortex, inferior parietal lobe, medial occipital cortex, and lunate cortex. The calcarine gyrus was thicker in these children than in controls (Fig. 1, Table 2).

Diffusivity

The FA values of ORs in amblyopia were significantly lower than in controls (Fig. 2). The number of reconstructed OR fibers did not differ significantly between the two groups (Table 3). Also, there was no significant difference in the mean FA value, voxel value, and number of ORs between the bilateral ORs in amblyopic children and controls (Table 3).

Correlations of OR Integrity with Cortical Thickness in Regions of Interest

There were positive correlations between cortical thickness and the FA values of ORs in the medial lingual cortex (MLP) ($r^2 = 0.331$, $P = 0.0253$), superior occipital gyrus (SO) ($r^2 = 0.361$, $P = 0.0181$), and occipital temporal medial and lingual (OTML) cortex ($r^2 = 0.395$, $P = 0.0163$) in the left hemisphere; and in the lateral occipitotemporal gyrus (LOTG) ($r^2 = 0.448$, $P = 0.0091$), MLP ($r^2 = 0.365$, $P = 0.0174$), SO ($r^2 = 0.343$, $P = 0.0225$), and OTML ($r^2 = 0.492$, $P = 0.0079$) in the right hemisphere. There was a trend of positive correlations in the left LOTG ($r^2 = 0.302$, $P = 0.0341$) and middle occipital and lunate cortex (OML) ($r^2 = 0.272$, $P = 0.0469$) and the right OML ($r^2 = 0.273$, $P = 0.0457$). However, there was no significant correlation in the

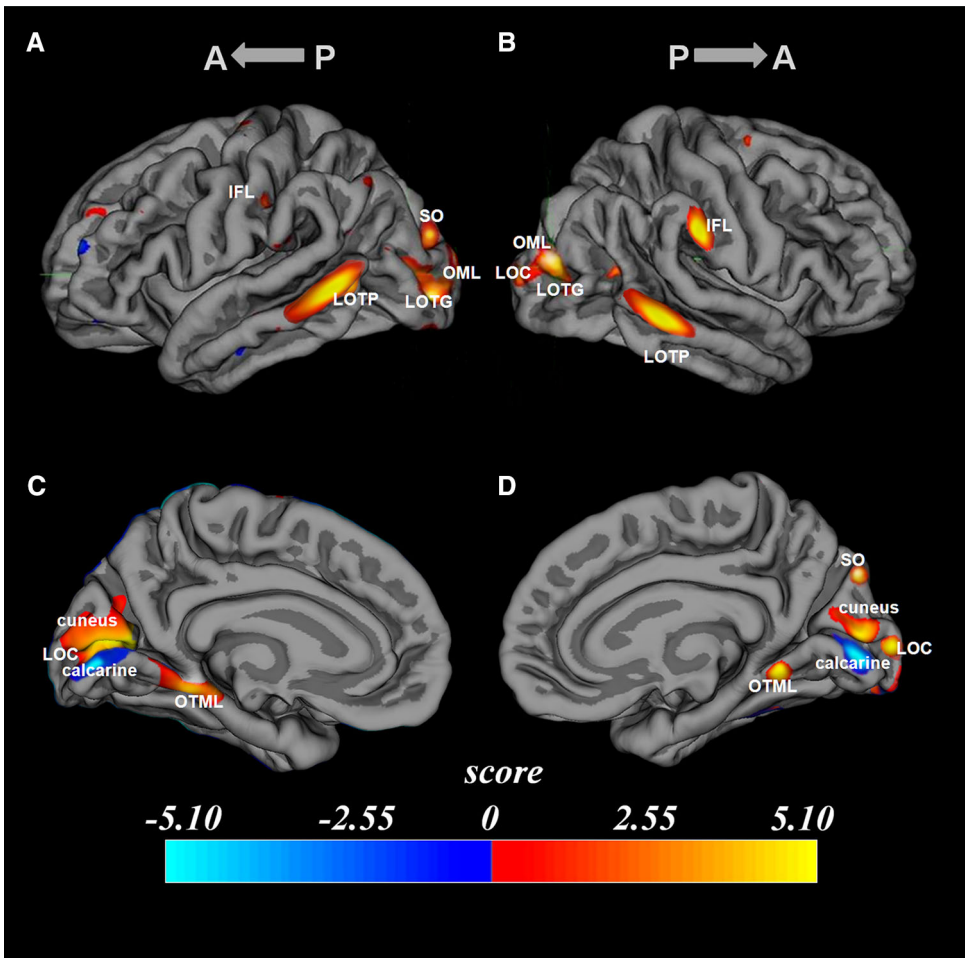

Fig. 1 Regions with alterations of cortical thickness in children with anisometropic amblyopia relative to normal controls. **A** Regions with significant cortical thickness changes in a lateral view of the left hemisphere with the inflated model. **B** Regions in a lateral view of the right hemisphere. **C** Regions in a medial view of the left hemisphere. **D** Regions in a medial view of the right hemisphere. The *color map* overlays the reconstruction image, age and gender effects were removed by regression, and thresholded at $P < 0.05$ corrected for multiple comparison. The color-code for T value is on a logarithmic scale of −5.1–5.1, shown below. Warmer colors (*positive values*) represent cortical thinning; cooler colors (*negative values*) represent cortical thickening.

following cortical regions: the inferior parietal lobe, calcarine gyrus, cuneus, lateral occipital cortex, and occipital temporal-parietal cortex (Fig. 3).

Discussion

Our main findings were that (1) the FA values of ORs in children with anisometropic amblyopia were significantly lower than in controls, but there was no significant difference in FA values between the bilateral ORs; (2) the cortical thickness was significantly lower in the bilateral occipital lobe, lingual gyrus, cuneus, and lunate cortex, and significantly higher in the calcarine cortex, in amblyopic children than in controls; and (3) there were significant correlations between FA value and average cortical thickness in the medial lingual cortex, lateral occipitotemporal gyrus, lateral, superior, and middle occipital cortex, and lunate cortex. All these results suggest that the reduced thickness in the visual cortex is due to OR damage in children with anisometropic amblyopia, reflecting projection impairments in their functional networks.

Decreased gray matter volume and density in different regions have been revealed by VBM [16, 40], but this method does not have specificity for highly convoluted structures of the cortex [41]. SBM is a recently-developed and highly reliable MRI-derived neuroanatomical measure, which overcomes the shortcomings of volume-based analysis, and is unaffected by voxel geometry [42]. In this study, we found thinning of the bilateral occipital lobe, lingual gyrus, cuneus, and lunate cortex in amblyopia. fMRI has also indicated that adults and children with amblyopia have functional deficits of the visual cortex [7]. From the electrophysiological perspective, in senescent individuals, the age-associated decline of selectivity of visual cortical neurons to spatial frequency might contribute to the decreased visual acuity [43]. Vision is relatively poorly developed at birth; normal acuity is achieved at about three years of age, given proper visual stimulation in the early months and years after birth [44]. If the stimulation is anomalous for the receptors, vision does not develop properly, leading to amblyopia [2]. It is well established that amblyopia is a failure of the cortical developmental process [45–48], although the exact extent of the visual cortex deficit is largely unknown. Previous

Table 2 Differences in cortical thickness between children with anisometropic amblyopia and controls

Brain regions	Anisometropic amblyopia mean (SD) (mm)	Normal control mean (SD) (mm)	*T* value	*P* value
Left hemisphere				
MLP	2.27 (0.14)	2.04 (0.06)	2.654	0.007
LOTG	1.75 (0.15)	1.47 (0.08)	3.479	0.002
Lateral occip	2.47 (0.19)	2.21 (0.15)	2.952	0.003
Cuneus	1.97 (0.28)	1.87 (0.10)	1.796	0.027
SO	2.22 (0.18)	2.13 (0.23)	1.579	0.034
IFL	2.03 (0.13)	1.93 (0.35)	1.794	0.031
OML	2.17 (0.21)	2.06 (0.22)	2.101	0.019
OTP	2.68 (0.18)	2.42 (0.11)	2.947	0.006
OTML	2.17 (0.10)	2.02 (0.13)	2.122	0.015
Calcarine	1.72 (0.16)	1.83 (0.21)	−2.077	0.024
Right hemisphere				
MLP	2.26 (0.17)	2.13 (0.39)	2.128	0.019
LOTG	1.69 (0.25)	1.68 (0.28)	1.371	0.049
Lateral occip	2.54 (0.13)	2.24 (0.26)	3.917	0.001
Cuneus	2.09 (0.29)	1.93 (0.26)	2.438	0.013
SO	2.17 (0.28)	2.10 (0.17)	1.541	0.039
IFL	2.08 (0.65)	1.82 (0.47)	2.534	0.007
OML	2.29 (0.13)	2.25 (0.41)	1.355	0.041
OTP	2.57 (0.15)	2.37 (0.14)	2.522	0.008
OTML	2.19 (0.13)	2.01 (0.16)	2.485	0.009
Calcarine	1.68 (0.15)	1.79 (0.27)	−1.925	0.025

Region abbreviations from FreeSurfer model: IFL, inferior parietal lobe; Lateral occip, lateral-occipital cortex; LOTG, lateral occipital temporal gyrus; LOTP, lateral occipital temporal cortex; MLP, medial lingual cortex; OML, middle occipital and lunate cortex; OTP, occipital temporal-parietal cortex OTML, occipital temporal medial and lingual; SO, superior occipital gyrus. $P < 0.05$ corrected for multiple comparisons, Two-sample t-test. Positive *T* value represents decreased cortical thickness and negative *T* value represents increased cortical thickness in anisometropic amblyopia compared to healthy children.

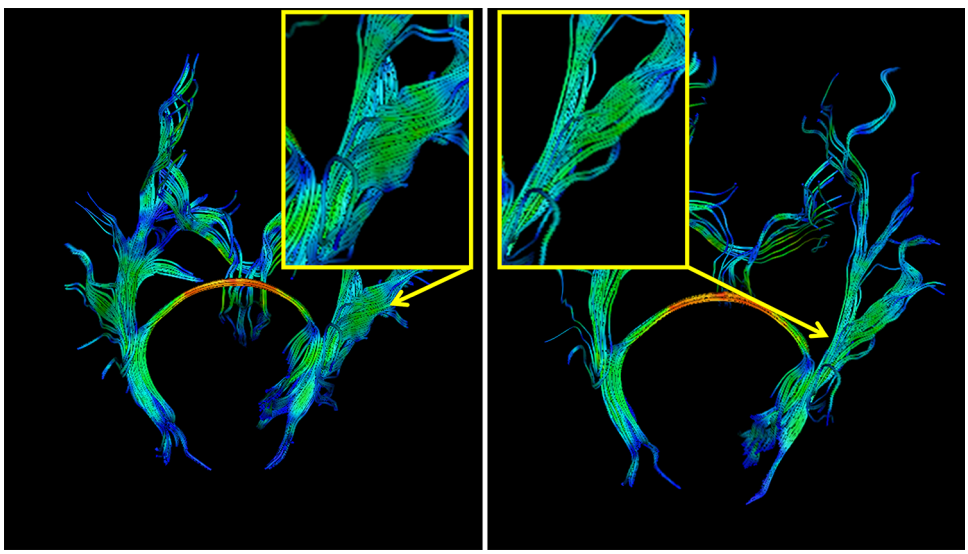

Fig. 2 Representative images showing high-resolution reconstruction of DTI fiber tracks of ORs. *Left panel* representative tracts of ORs of a healthy child, *right panel* representative tracts of ORs in a child with anisometropic amblyopia. *Inserts* show significant differences between the DTT reconstructed images in amblyopia relative to controls.

studies have shown that the thickness of visual cortex in blind patients can manifest compensatory thickening [41, 49]. The increased thickness of the calcarine sulcus in this study could reflect more visual stimulation in the primary visual cortex, and an increase in connectivity in this region.

Table 3 FAs, voxel values, and numbers of ORs from amblyopic children and controls, including ipsilateral and contralateral ORs

	FA values of ORs mean (SD)	Voxel values of ORs mean (SD)	Number of tracks* mean (SD)
Amblyopia	0.47 (0.05)	3093.03 (179.61)	826.24 (20.57)
Control	0.52 (0.06)	3179.15 (127.59)	840.71 (18.12)
T	3.041	1.148	1.291
P	0.015	0.824	0.851
IORsA	0.48 (0.05)	3071.09 (171.09)	827.88 (21.28)
CORsA	0.46 (0.04)	2988.62 (198.62)	837.13 (18.79)
T	1.314	1.104	1.384
P	0.831	0.819	0.794
IORsC	0.52 (0.07)	3217.13 (114.58)	849.34 (19.91)
CORsC	0.51 (0.05)	3192.71 (146.27)	833.82 (17.63)
T	1.411	1.092	1.299
P	0.772	0.891	0.813

* Number of tracks of ORs longer than the mean length (43.24 mm). FA, fractional anisotropy; ORs, optic radiations; IORsA, ipsilateral ORs in amblyopia group; CORsA, contralateral ORs in amblyopia group; IORsC, ipsilateral ORs in control group; CORsC, contralateral ORs in control group. *P* and *T* values were obtained by a two-sample *t* test.

It is believed that FA in DTI can provide microstructural information about white matter development [22]. Furthermore, DTT enables extraction of the trajectories of certain fiber tracts *in vivo*. Current DTI results show that in children with anisometropic amblyopia, the FA values of ORs are significantly lower than in controls. This has been verified in a similar investigation in the previous study, which also found more voxels in the posterior ORs of controls than in the amblyopic children [50]. Sampling of high-spatial-frequency components of visual stimuli in visual cortex revealed the main dysfunction in anisometropic amblyopia [51]. A reduction of FA implies either a difference of such fiber architecture such as axon density, size, orientation, and internal structure, or a difference in myelination of the fibers. In our study, tractography showed a reduction of FA in the LGN of bilateral ORs of amblyopic children, which indicated that the controls had better OR development. It is known that children's brains undergo an extended period of postnatal maturation, with increasing white matter as well as progression of myelination. Recent advances in neuroscience have provided evidence of an effect of training on white matter development [52]. It has been routinely reported that visual-evoked potentials in human amblyopes are reduced and distorted, indicating dysfunction of the visual pathway [53, 54]. In animal models, it has been demonstrated that neuronal activity triggers the induction of myelination and that myelination of the optic nerve is decelerated when animals are reared in darkness [55]. As such, the anomalous development of ORs found in our study may result from abnormal neuronal signals and weak connections. Another explanation for the current results may be that the myelination of ORs was affected by the low acuity of the amblyopic eye; this has also been found in another study [56]. It might be associated with the fact that the ORs receive visual inputs from both eyes. Anisotropic diffusion in white matter may be due to the effect of myelination, axonal thickness, amount of parallel organization of axons, or a combination of these factors [57]. In a previous study, the fiber tract organization was found to be positively correlated with practice, and the increased myelination induced by neuronal activity in fiber tracts during training contributes to the increase in FA [24]. Therefore, well-developed ORs would be expected to have higher FA values, and lower FAs in bilateral ORs indicate that children with anisometropic amblyopia exhibit abnormalities in both ORs, which has been demonstrated previously [50].

Because the ORs are bidirectional, we believe that their underdevelopment in amblyopia is probably related to changes in both the visual cortex and LGN. DTI and fMRI have revealed that the FA values of ORs are positively correlated with functional activity of the visual cortex [28], and the functional deficit in amblyopia is accompanied by changes in the cortical volume of the occipital lobe [58]. These results imply that the impairment of white matter integrity associated with dysfunction-related cerebral cortex, i.e., the visual cortex, may accompany structural deficit in the visual cortex. The ability of amblyopia patients to process visual impulses from the LGN is reduced, which directly affects OR white matter development, leading to a decreased FA value, meanwhile causing dysfunction of the visual cortex. However, the extent to which OR integrity changes with the thickness of the visual cortex in

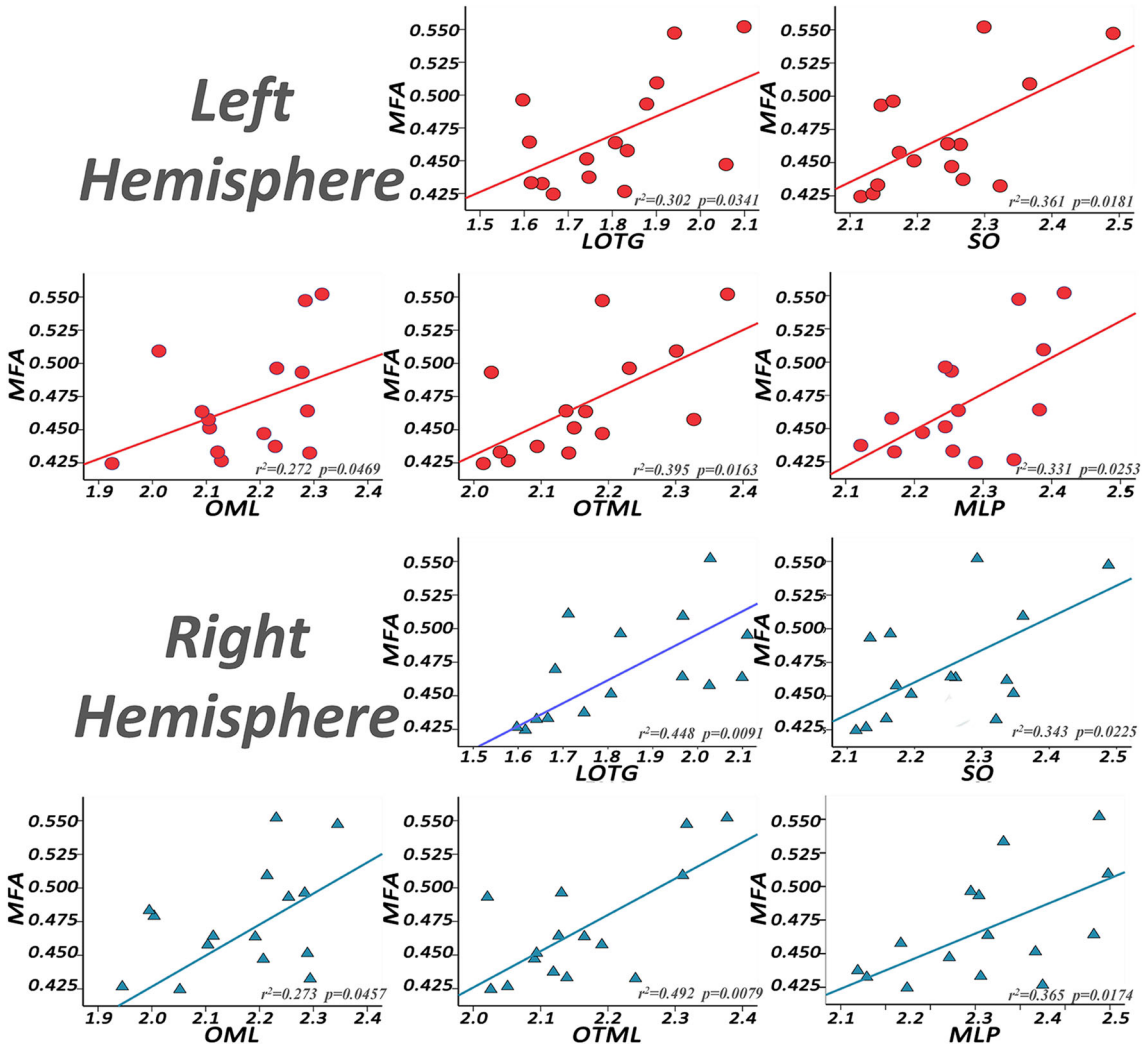

Fig. 3 Correlations of OR fractional anisotropy with mean cortical thickness in regions with significant cortical changes in patients with anisometropic amblyopia. *X-axes* mean cortical thickness, *Y-axis* mean FAs of ORs (Pearson's correlation analysis; r and p values at *lower right*). MLP, medial lingual cortex; LOTG, lateral occipital temporal gyrus; SO, superior occipital gyrus; OML, middle occipital and lunate cortex; OTML medial occipital temporal cortex.

amblyopia was unclear. This study is the first to investigate the relationship between deficits in the integrity of ORs and cortical thinning in anisometropic amblyopia. We found that the OR-related visual cortex changes were all in the V1 area (LOTG, OML, SO, OTML, and MLP). But cortical thinning in other regions (IFL, cuneus, and LOTP) was not associated with the impairment of OR integrity. In patients with anisometropic amblyopia, the activation by higher-spatial-frequency stimuli in visual cortex is reduced [51]. Visual input can be processed separately by different types of visual cortical neurons [59], so the related OR fibers may experience dysfunction, causing the subregional cortical thinning in the related visual cortex. The detailed mechanism still needs further studies investigation. In this study, the reduction in OR FA value was not correlated with reduced cortical thickness in some regions. A possible explanation is that the cortical thickness changes in those regions may be secondary to deficits in the primary visual cortex, in other words, they are compensative effects for neuron agenesis. It is also possible that cortical thickness changes in the inferior parietal lobe are caused not only by the reduction of visual information from the retina, but also by changes in cognitive activities, such as the basic visual sensation and perception [28].

The present work has several limitations, which we plan to address in future studies. First, the sample size is small. We had only 15 children with anisometropic amblyopia and 15 controls, which may hinder the detection of subtle cortical thinning. Second, we only studied patients with anisometropic amblyopia but not those with strabismic amblyopia. Comparison between the two types of amblyopia will help better understand their pathogenic

mechanisms. Third, the ROI approach is not optimal to map the whole-brain white matter. Partial volume effects on gray matter and/or CSF in the white matter may blur DTI measures [55]. A histogram-based or voxel-based statistical approach may overcome the partial volume effects. However, these methods, which require a smoothing step and a normalization scheme, might limit the sensitivity of anisotropic measurements. Fourth, we did not investigate the correlations among OR integrity, cortical thickness, and visual acuity loss or duration of amblyopia; we will do these in further work.

In conclusion, we report impaired OR integrity and cortical thickness reduction within the visual cortex in anisometropic amblyopia. The reductions of thickness in subregions of visual cortex were correlated with impairment of OR fiber integrity. These findings indicate that amblyopia can cause anomalous development in both ORs and visual cortex.

Acknowledgments This work was supported by the National Natural Science Foundation of China (30872717).

References

1. Shimko JF. Binocular Vision and Ocular Motility Theory and Management of Strabismus Gunter K. vonNoorden, M.D.; Emilio C. Campos, M.D. Mosby Inc., Sixth Edition 2002, $149.00; 631 pages, 315 illustrations. Am Orthopt J 2001, 51: 161–162.
2. Kutschke PJ, Scott WE, Keech RV. Anisometropic amblyopia. Ophthalmology 1991, 98: 258–263.
3. Gingras G, Mitchell DE, Hess RF. The spatial localization deficit in visually deprived kittens. Vision Res 2005, 45: 975–989.
4. Schmidt KE, Singer W, Galuske RA. Processing deficits in primary visual cortex of amblyopic cats. J Neurophysiol 2004, 91: 1661–1671.
5. Dasenbrock HH, Smith SA, Ozturk A, Farrell SK, Calabresi PA, Reich DS. Diffusion tensor imaging of the optic tracts in multiple sclerosis: association with retinal thinning and visual disability. J Neuroimaging 2011, 21: e41–49.
6. Schoth F, Krings T. Diffusion-tensor imaging in septo-optic dysplasia. Neuroradiology 2004, 46: 759–763.
7. Du H, Xie B, Yu Q, Wang J. Occipital lobe's cortical thinning in ametropic amblyopia. Magn Reson Imaging 2009, 27: 637–640.
8. Choi MY, Lee DS, Hwang JM, Choi DG, Lee KM, Park KH, *et al.* Characteristics of glucose metabolism in the visual cortex of amblyopes using positron-emission tomography and statistical parametric mapping. J Pediatr Ophthalmol Strabismus 2002, 39: 11–19.
9. Imamura K, Richter H, Fischer H, Lennerstrand G, Franzen O, Rydberg A, *et al.* Reduced activity in the extrastriate visual cortex of individuals with strabismic amblyopia. Neurosci Lett 1997, 225: 173–176.
10. Anderson SJ, Swettenham JB. Neuroimaging in human amblyopia. Strabismus 2006, 14: 21–35.
11. Davis AR, Sloper JJ, Neveu MM, Hogg CR, Morgan MJ, Holder GE. Electrophysiological and psychophysical differences between early- and late-onset strabismic amblyopia. Invest Ophthalmol Vis Sci 2003, 44: 610–617.
12. Li ML, Xiang B, Li YF, Hu X, Wang Q, Guo WJ, *et al.* Morphological changes in gray matter volume correlate with catechol-O-methyl transferase gene Val158Met polymorphism in first-episode treatment-naive patients with schizophrenia. Neurosci Bull 2015, 31: 31–42.
13. Ma M, Qian C, Li Y, Zuo Z, Liu Z. Setup and data analysis for functional magnetic resonance imaging of awake cat visual cortex. Neurosci Bull 2013, 29: 588–602.
14. Lerner Y, Pianka P, Azmon B, Leiba H, Stolovitch C, Loewenstein A, *et al.* Area-specific amblyopic effects in human occipitotemporal object representations. Neuron 2003, 40: 1023–1029.
15. Conner IP, Odom JV, Schwartz TL, Mendola JD. Monocular activation of V1 and V2 in amblyopic adults measured with functional magnetic resonance imaging. J AAPOS 2007, 11: 341–350.
16. Mendola JD, Conner IP, Roy A, Chan ST, Schwartz TL, Odom JV, *et al.* Voxel-based analysis of MRI detects abnormal visual cortex in children and adults with amblyopia. Hum Brain Mapp 2005, 25: 222–236.
17. Ridgway GR, Henley SM, Rohrer JD, Scahill RI, Warren JD, Fox NC. Ten simple rules for reporting voxel-based morphometry studies. NeuroImage 2008, 40: 1429–1435.
18. van der Kouwe AJ, Benner T, Salat DH, Fischl B. Brain morphometry with multiecho MPRAGE. NeuroImage 2008, 40: 559–569.
19. Ghosh SS, Kakunoori S, Augustinack J, Nieto-Castanon A, Kovelman I, Gaab N, *et al.* Evaluating the validity of volume-based and surface-based brain image registration for developmental cognitive neuroscience studies in children 4 to 11 years of age. NeuroImage 2010, 53: 85–93.
20. Kim H, Besson P, Colliot O, Bernasconi A, Bernasconi N. Surface-based vector analysis using heat equation interpolation: a new approach to quantify local hippocampal volume changes. Med Image Comput Comput Assist Interv 2008, 11: 1008–1015.
21. Berman JI, Mukherjee P, Partridge SC, Miller SP, Ferriero DM, Barkovich AJ, *et al.* Quantitative diffusion tensor MRI fiber tractography of sensorimotor white matter development in premature infants. NeuroImage 2005, 27: 862–871.
22. Hermoye L, Saint-Martin C, Cosnard G, Lee SK, Kim J, Nassogne MC, *et al.* Pediatric diffusion tensor imaging: normal database and observation of the white matter maturation in early childhood. NeuroImage 2006, 29: 493–504.
23. Filippi CG, Lin DD, Tsiouris AJ, Watts R, Packard AM, Heier LA, *et al.* Diffusion-tensor MR imaging in children with developmental delay: preliminary findings. Radiology 2003, 229: 44–50.
24. Bengtsson SL, Nagy Z, Skare S, Forsman L, Forssberg H, Ullen F. Extensive piano practicing has regionally specific effects on white matter development. Nat Neurosci 2005, 8: 1148–1150.
25. Song HY, Qi S, Tang HH, Yu FJ, Liu LQ. MR DTI and DTT study on the development of optic radiation in patients with anisometropia amblyopia. Sichuan Da Xue Xue Bao Yi Xue Ban 2010, 41: 648–651.
26. Reinges MH, Schoth F, Coenen VA, Krings T. Imaging of postthalamic visual fiber tracts by anisotropic diffusion weighted MRI and diffusion tensor imaging: principles and applications. Eur J Radiol 2004, 49: 91–104.
27. Yamamoto T, Yamada K, Nishimura T, Kinoshita S. Tractography to depict three layers of visual field trajectories to the calcarine gyri. Am J Ophthalmol 2005, 140: 781–785.
28. Toosy AT, Ciccarelli O, Parker GJ, Wheeler-Kingshott CA, Miller DH, Thompson AJ. Characterizing function-structure relationships in the human visual system with functional MRI and diffusion tensor imaging. NeuroImage 2004, 21: 1452–1463.
29. Webber AL, Wood J. Amblyopia: prevalence, natural history, functional effects and treatment. Clin Exp Optom 2005, 88: 365–375.

30. Fischl B, Dale AM. Measuring the thickness of the human cerebral cortex from magnetic resonance images. Proc Natl Acad Sci U S A 2000, 97: 11050–11055.
31. Du AT, Schuff N, Kramer JH, Rosen HJ, Gorno-Tempini ML, Rankin K, *et al.* Different regional patterns of cortical thinning in Alzheimer's disease and frontotemporal dementia. Brain 2007, 130: 1159–1166.
32. Bischoff-Grethe A, Ozyurt IB, Busa E, Quinn BT, Fennema-Notestine C, Clark CP, *et al.* A technique for the deidentification of structural brain MR images. Hum Brain Mapp 2007, 28: 892–903.
33. Pantazis D, Joshi A, Jiang J, Shattuck DW, Bernstein LE, Damasio H, *et al.* Comparison of landmark-based and automatic methods for cortical surface registration. NeuroImage 2010, 49: 2479–2493.
34. Fischl B, Liu A, Dale AM. Automated manifold surgery: constructing geometrically accurate and topologically correct models of the human cerebral cortex. IEEE Trans Med Imaging 2001, 20: 70–80.
35. Wedeen VJ, Wang RP, Schmahmann JD, Benner T, Tseng WY, Dai G, *et al.* Diffusion spectrum magnetic resonance imaging (DSI) tractography of crossing fibers. NeuroImage 2008, 41: 1267–1277.
36. Bazarian JJ, Zhong J, Blyth B, Zhu T, Kavcic V, Peterson D. Diffusion tensor imaging detects clinically important axonal damage after mild traumatic brain injury: a pilot study. J Neurotrauma 2007, 24: 1447–1459.
37. Chang MC, Kim SH, Kim OL, Bai DS, Jang SH. The relation between fornix injury and memory impairment in patients with diffuse axonal injury: a diffusion tensor imaging study. NeuroRehabilitation 2010, 26: 347–353.
38. Galban CJ, Maderwald S, Uffmann K, Ladd ME. A diffusion tensor imaging analysis of gender differences in water diffusivity within human skeletal muscle. NMR Biomed 2005, 18: 489–498.
39. Benjamini Y, Yekutieli D. The Control of the false discovery rate in multiple testing under dependency. Ann Stat 2001, 29: 1165–1188.
40. Xiao JX, Xie S, Ye JT, Liu HH, Gan XL, Gong GL, *et al.* Detection of abnormal visual cortex in children with amblyopia by voxel-based morphometry. Am J Ophthalmol 2007, 143: 489–493.
41. Makris N, Kaiser J, Haselgrove C, Seidman LJ, Biederman J, Boriel D, *et al.* Human cerebral cortex: a system for the integration of volume- and surface-based representations. NeuroImage 2006, 33: 139–153.
42. Wonderlick JS, Ziegler DA, Hosseini-Varnamkhasti P, Locascio JJ, Bakkour A, van der Kouwe A, *et al.* Reliability of MRI-derived cortical and subcortical morphometric measures: effects of pulse sequence, voxel geometry, and parallel imaging. NeuroImage 2009, 44: 1324–1333.
43. Hua GP, Shi XM, Zhou J, Peng QS, Hua TM. Decline of selectivity of V1 neurons to visual stimulus spatial frequencies in old cats. Neurosci Bull 2011, 27: 9–14.
44. Li C, Cheng L, Yu Q, Xie B, Wang J. Relationship of visual cortex function and visual acuity in anisometropic amblyopic children. Int J Med Sci 2012, 9: 115–120.
45. Thompson B, Villeneuve MY, Casanova C, Hess RF. Abnormal cortical processing of pattern motion in amblyopia: evidence from fMRI. NeuroImage 2012, 60: 1307–1315.
46. Li X, Dumoulin SO, Mansouri B, Hess RF. Cortical deficits in human amblyopia: their regional distribution and their relationship to the contrast detection deficit. Invest Ophthalmol Vis Sci 2007, 48: 1575–1591.
47. Kubova Z, Kuba M, Juran J, Blakemore C. Is the motion system relatively spared in amblyopia? Evidence from cortical evoked responses. Vision Res 1996, 36: 181–190.
48. Ikeda H, Tremain K. Amblyopia and cortical binocularity. Trans Ophthalmol Soc U K 1980, 100: 450–452.
49. Jiang J, Zhu W, Shi F, Liu Y, Li J, Qin W, *et al.* Thick visual cortex in the early blind. J Neurosci 2009, 29: 2205–2211.
50. Xie S, Gong GL, Xiao JX, Ye JT, Liu HH, Gan XL, *et al.* Underdevelopment of optic radiation in children with amblyopia: a tractography study. Am J Ophthalmol 2007, 143: 642–646.
51. Lee KM, Lee SH, Kim NY, Kim CY, Sohn JW, Choi MY, *et al.* Binocularity and spatial frequency dependence of calcarine activation in two types of amblyopia. Neurosci Res 2001, 40: 147–153.
52. Skup M, Dwornik A, Macias M, Sulejczak D, Wiater M, Czarkowska-Bauch J. Long-term locomotor training up-regulates TrkB(FL) receptor-like proteins, brain-derived neurotrophic factor, and neurotrophin 4 with different topographies of expression in oligodendroglia and neurons in the spinal cord. Exp Neurol 2002, 176: 289–307.
53. Sokol S, Hansen VC, Moskowitz A, Greenfield P, Towle VL. Evoked potential and preferential looking estimates of visual acuity in pediatric patients. Ophthalmology 1983, 90: 552–562.
54. Sokol S. Abnormal evoked potential latencies in amblyopia. Br J Ophthalmol 1983, 67: 310–314.
55. Demerens C, Stankoff B, Logak M, Anglade P, Allinquant B, Couraud F, *et al.* Induction of myelination in the central nervous system by electrical activity. Proc Natl Acad Sci U S A 1996, 93: 9887–9892.
56. Lerner Y, Hendler T, Malach R, Harel M, Leiba H, Stolovitch C, *et al.* Selective fovea-related deprived activation in retinotopic and high-order visual cortex of human amblyopes. NeuroImage 2006, 33: 169–179.
57. Beaulieu C. The basis of anisotropic water diffusion in the nervous system - a technical review. NMR Biomed 2002, 15: 435–455.
58. Lv B, He H, Li X, Zhang Z, Huang W, Li M, *et al.* Structural and functional deficits in human amblyopia. Neurosci Lett 2008, 437: 5–9.
59. Super H. Cognitive processing in the primary visual cortex: from perception to memory. Rev Neurosci 2002, 13: 287–298.